Expression Profile of the Matricellular Protein Osteopontin in Primary Open-Angle Glaucoma and the Normal Human Eye

Uttio Roy Chowdhury,[1] *Seung-Youn Jea,*[2] *Dong-Jin Oh,*[2] *Douglas J. Rhee,*[2] *and Michael P. Fautsch*[1]

Purpose. To characterize the role of osteopontin (OPN) in primary open-angle glaucoma (POAG) and normal eyes.

Methods. OPN quantification was performed by enzyme-linked immunosorbent assay in aqueous humor (AH) obtained from human donor eyes (POAG and normal) and surgical samples (POAG and elective cataract removal). OPN expression and localization in whole eye tissue sections and primary normal human trabecular meshwork (NTM) cells were studied by Western blot and immunohistochemistry. Latanoprost-free acid (LFA)–treated NTM cells were analyzed for *OPN* gene and protein expression. Intraocular pressure was measured by tonometry, and central corneal thickness was measured by optical coherence tomography in young $OPN^{-/-}$ and wild-type mice.

Results. OPN levels were significantly reduced in donor POAG AH compared with normal AH (0.54 ± 0.18 ng/μg [$n = 8$] vs. 0.77 ± 0.23 ng/μg [$n = 9$]; $P = 0.039$). A similar trend was observed in surgical AH (1.05 ± 0.31 ng/μg [$n = 20$] vs. 1.43 ± 0.88 ng/μg [$n = 20$]; $P = 0.083$). OPN was present in the trabecular meshwork, corneal epithelium and endothelium, iris, ciliary body, retina, vitreous humor, and optic nerve. LFA increased *OPN* gene expression, but minimal change in OPN protein expression was observed. No difference in intraocular pressure (17.5 ± 2.0 mm Hg [$n = 56$] vs. 17.3 ± 1.9 mm Hg [$n = 68$]) but thinner central corneal thickness (91.7 ± 3.6 μm [$n = 50$] vs. 99.2 ± 5.5 μm [$n = 70$]) was noted between $OPN^{-/-}$ and wild-type mice.

Conclusions. OPN is widely distributed in the human eye and was found in lower concentrations in POAG AH. Reduction of OPN in young mice does not affect IOP. (*Invest Ophthalmol Vis Sci.* 2011;52:6443–6451) DOI:10.1167/iovs.11-7409

Elevated intraocular pressure (IOP) in primary open-angle glaucoma (POAG) is caused by increased outflow resistance within the trabecular meshwork, the tissue that drains most of the aqueous humor (AH) from the anterior segment of the human eye.[1] Changes that occur within the trabecular cells, in protein secretions, or within the extracellular matrix have been identified as the most likely causes for increased outflow resistance in POAG.[2,3] Traditionally, standard treatment for POAG has focused on reducing IOP surgically, through medications, or both. Pharmaceutical agents such as the prostaglandin analogs (e.g., latanoprost) enhance the flow of AH by stimulating extracellular matrix (ECM) turnover by expression changes of matrix metalloproteinases, tissue inhibitor of metalloproteinases, and matricellular proteins.[4–7]

Matricellular proteins are nonstructural ECM proteins that regulate cellular function and matrix production by interacting with cellular receptors, growth factors, and cytokines. Matricellular proteins are involved in a wide range of cell modulatory functions, including cell adhesion, migration, survival, and apoptosis.[8–11] Several members of the matricellular protein family have been identified as potential regulators of aqueous outflow resistance. For example, mice lacking the matricellular protein SPARC (secreted protein, acidic and rich in cysteine) have lower IOP than wild-type controls.[12] Hevin, a matricellular protein with homology to SPARC, interacts with a mutant form of the glaucoma-associated protein myocilin.[13] Thrombospondin 1, a multifunctional matricellular protein, is elevated at the mRNA level in primary cultures of lamina cribrosa cells obtained from POAG patients and is also a key activator of transforming growth factor beta (TGFβ), which is elevated in 50% of POAG AH.[14–19] Tenascin C, another member of the matricellular protein family, is upregulated in response to mechanical stretch and has been shown to alter cell shape, migration, and adhesion.[20–22] However, though somewhat defined, the role of matricellular proteins in IOP regulation and glaucoma is still relatively unknown.

Osteopontin (OPN), another member of the matricellular protein family, is a key regulator of ECM mineralization and bone formation, is considered a strong marker of calcification, vascular diseases (e.g., atherosclerosis), and biomineralization, and is a prognostic marker for inflammatory heart diseases.[23–26] OPN is associated with a wide range of biological processes, including cell adhesion, migration, cell survival, activation of immune cells, and ECM remodeling, and is an inhibitor of vascular calcification.[8,9,11,27–29] In the eye, OPN modulates wound healing and neovascularization in the mouse cornea, controls epithelial-mesenchymal transition in the mouse lens, and is upregulated in rat retinal ganglion cells in response to excitotoxic and ischemic injury.[30–33] In the normal trabecular meshwork, the expression of *OPN* mRNA and several other genes associated with calcification inhibition indicates a possible role of these molecules in maintaining a healthy trabecular meshwork.[34–38] Imbalance of these inhibitors may lead to a less pliable trabecular meshwork that even-

From the [1]Department of Ophthalmology, Mayo Clinic, Rochester, Minnesota; and the [2]Department of Ophthalmology, Massachusetts Eye and Ear Infirmary, Harvard Medical School, Boston, Massachusetts.

Supported in part by National Institutes of Health Research Grants EY 07065 (MPF), EY 15736 (MPF), and EY 019654 (DJR); the Mayo Foundation; and Research to Prevent Blindness (Lew R. Wasserman Merit Award [MPF] and an unrestricted grant [Department of Ophthalmology, Mayo Clinic]).

Submitted for publication February 16, 2011; revised June 9, 2011; accepted June 28, 2011.

Disclosure: **U.R. Chowdhury**, None; **S.-Y. Jea**, None; **D.-J. Oh**, None; **D.J. Rhee**, None; **M.P. Fautsch**, None

Corresponding author: Michael P. Fautsch, Department of Ophthalmology, Mayo Clinic, 200 First Street SW, Rochester, MN 55905; fautsch.michael@mayo.edu.

tually may affect outflow and IOP. This is consistent with increased trabecular meshwork stiffness in glaucoma.[39]

We recently identified OPN as one of the most abundant proteins in human AH.[40] Given the high level of OPN expression in AH, its potential role as an inhibitor of tissue calcification, and the involvement of other matricellular proteins in IOP regulation, we evaluated the distribution profile of OPN in human ocular tissues and compared OPN concentrations between normal and POAG AH samples. In addition, OPN expression was analyzed in normal human trabecular meshwork (NTM) cells after latanoprost-free acid (LFA) treatment to determine whether OPN levels were influenced by IOP-lowering medications. Finally, the role of OPN in IOP regulation was examined in $OPN^{-/-}$ mice.

Materials and Methods

Collection of Eye Tissues and Fluids

The protocol for collection of human AH was approved by the Mayo Clinic Institutional Review Board and conforms to tenets of the Declaration of Helsinki.

Donor. POAG and normal human donor eyes were obtained from the Minnesota Lions Eye Bank within 12 hours of death. AH was obtained from the anterior chamber with a tuberculin syringe placed parallel to the cornea and was inserted above the limbus. The trabecular meshwork, retina, iris, and optic nerve were dissected and stored at −80°C. Vitreous humor was isolated and centrifuged at 3000*g* for 10 minutes, and the supernatant was collected and stored at −80°C. Total protein concentrations of all AH, vitreous humor, and tissue lysates were determined using the Bradford protein assay (Bio-Rad, Hercules, CA).

Surgical. At the time of trabeculectomy (POAG) or elective cataract surgery, a 30-gauge needle was inserted into the mid-anterior chamber through a paracentesis tract. AH was slowly aspirated until the anterior chamber began to shallow. AH was transferred to a vial and immediately placed in liquid nitrogen. Control samples were obtained from patients with no identified eye disorders other than senile cataract. Neither POAG nor elective cataract AH samples were obtained from patients treated with systemic or topical steroids before surgery.

Quantification of OPN in AH and Conditioned Media

OPN was quantified in donor POAG ($n = 8$), donor normal ($n = 9$), surgical POAG ($n = 20$), and elective cataract surgery ($n = 20$) using a human OPN enzyme-linked immunosorbent assay (ELISA) kit (Quantikine; R&D Systems, Minneapolis, MN; detection limits ≥6 pg/mL). Two microliters of each AH sample was diluted 50-fold with calibrator diluent, mixed with 100 μL assay diluent, and incubated for 2 hours at room temperature in individual microtiter plate wells coated with OPN monoclonal antibody. Each sample was washed three times with 400 μL wash buffer and incubated with an enzyme-linked polyclonal antibody for 2 hours at room temperature. Substrate solution was added to the bound antigen-antibody-enzyme complex, and fluorescence was calculated at 450 nm (with 540 nm as reference wavelength) on a microplate reader (Infinite M200; Tecan Systems, Inc., San Jose, CA). Concentrations of OPN in POAG and normal samples were established from a standard curve generated using several known concentrations of recombinant human OPN.

For OPN quantification, conditioned media containing 10% FBS was concentrated 10-fold using ultrafiltration spin columns (Vivaspin 6; Sartorius Stedim Biotech GmbH, Goettingen, Germany). Concentrated conditioned media (50 μL) were used for OPN quantification using the human OPN ELISA kit (Quantikine; R&D Systems) as described.

Western Blot Analysis of Human Eye Tissues and AH

Various eye tissues dissected from donor eyes were placed in lysis buffer (50 mM Tris, pH 8.0, 0.5% sodium dodecyl sulfate, 0.5% Triton X-100, 137 mM NaCl, 3 mM KCl, 8 mM Na_2HPO_4-$7H_2O$, 1 mM KH_2PO_4, protease inhibitors [Roche, Indianapolis, IN])[41] and homogenized using a rotor stator homogenizer (Polytron; Kinematica, Lucerne, Switzerland). Tissue lysates (15 μg) or AH volume containing 15 μg total protein were mixed in equal proportions with 2× Laemmli buffer, boiled, and separated on 4% to 15% SDS-PAGE gradient gels (Bio-Rad). Proteins were transferred to polyvinylidene difluoride membrane (Millipore, Billerica, MA) in 1× transfer buffer (50 mM Tris, 384 mM glycine, 0.01% SDS, 20% methanol). Membranes were blocked in 20 mM Tris (pH 7.5), 150 mM NaCl, 0.05% Tween-20, and 2% nonfat evaporated milk. Blots were probed with rabbit polyclonal anti–human OPN (Sigma-Aldrich, St. Louis, MO), mouse monoclonal anti–human GAPDH (Novus Biologicals, Littleton, CO), or mouse monoclonal anti–human serum albumin (Abcam, Cambridge, MA) antibodies, followed by a secondary horseradish peroxidase-linked anti–rabbit or anti–mouse antibody (GE Healthcare, Piscataway, NJ). Antibody/antigen complexes were detected using ECL Western blot signal detection reagent (GE Healthcare). Kodak film was used to visualize the protein signals (BioMax XAR; Eastman Kodak, Rochester, NY). Each film was digitized with a photographic scanner (Perfection 2400; Epson, Long Beach, CA). The band intensities in Western blot analysis were normalized to GAPDH (cell lysates) or human serum albumin (in AH) and quantified using ImageJ software (developed by Wayne Rasband, National Institutes of Health, Bethesda, MD; available at http://rsb.info.nih.gov/ij/index.html).

Immunohistochemistry and Confocal Microscopy

A human donor eye (81-year-old man) was immersion fixed in 10% neutral buffered formalin within 15 hours of death, dehydrated in a graded series of ethanol (75%, 85%, 95%, and 100%), and embedded in paraffin. Sections (5 μm) were mounted on glass slides (Superfrost/Plus; Fisher, Pittsburgh, PA) and baked at 60°C for 2 hours. For immunohistochemistry, tissue sections were deparaffinized in xylene and rehydrated in a graded series of ethanol (100%, 95%, 80%, 70%) followed by incubation in phosphate-buffered saline. Antigens were retrieved by incubating sections in 1 mM EDTA (pH 8.0) at 95°C for 30 minutes.[42] Tissue sections were blocked in phosphate-buffered saline containing 3% bovine serum albumin and 0.1% Triton X-100 and probed with mouse anti–human OPN monoclonal antibody (R&D Systems). Alexa Fluor 488–conjugated goat anti–mouse immunoglobulin was used as a secondary antibody (Molecular Probes, Eugene, OR). Sections were mounted in mounting medium (Vectashield/DAPI; Vector Laboratories, Burlingame, CA) and examined on a confocal laser microscope (Zeiss 510; Carl Zeiss, Thornwood, NY). Image capture of eye tissues and corresponding controls was performed using the same digital settings.

Enzymatic Deglycosylation of AH

An enzymatic protein deglycosylation kit (Sigma-Aldrich) was used for complete removal of O- and N-linked glycosides from AH proteins in accordance with the manufacturer's instructions. Briefly, 25 μg AH total protein was denatured at 100°C for 5 minutes in the presence of 1× reaction buffer and 2.5 μL denaturation solution in a final volume of 30 μL. The reaction mix was cooled to room temperature, and a panel of five different glycosidases (PNGase F, O-glycosidase, α-2(3,6,8,9)neuraminidase, β(1–4)galactosidase and β-N-acetylglucosaminidase) was added with 2.5 μL nonionic surfactant (Triton X-100; Sigma-Aldrich). The reaction mix was incubated for 3 hours at 37°C. After incubation, 35 μL reaction mixture was combined with 5× Laemmli buffer, boiled, and separated on 4% to 15% SDS-PAGE gradient gels. Proteins were transferred to polyvinylidene difluoride membrane and probed with OPN antibody, as described.

Primary Culture of Human Trabecular Meshwork Cells

Three primary human NTM cell lines derived from independent donor eyes (20- and 46-year-old women; 1-year-old boy) were isolated as described previously.[43] Briefly, trabecular meshwork tissue was dissected from human donor eyes and digested with collagenase A (Worthington Biochemical Corporation, Lakewood, NJ). The cells were pelleted, resuspended in Dulbecco's modified Eagle's medium (DMEM; Mediatech, Inc., Herndon, VA), and supplemented with 10% fetal bovine serum (FBS; Cellgro, Manassas, VA) and penicillin-streptomycin (100 U/mL final concentration; Invitrogen, Carlsbad, CA). Cells were placed in a six-well plate and were grown to confluence at 37°C and 5% CO_2. Cells from passages 3 to 7 were used for experiments performed in this study.

LFA Treatment of NTM Cell Cultures

LFA was purchased as a solution in methyl acetate from Cayman Chemical (Ann Arbor, MI). For use in the experiments, methyl acetate was evaporated under a gentle stream of nitrogen, and LFA was reconstituted in ethanol purged with nitrogen at a concentration of 10^{-4} M. The stock solution of LFA was diluted in DMEM with or without 10% FBS to a final working concentration of 10^{-7} M.

Primary human NTM cell lines ($n = 3$) were grown to confluence in six-well plates containing DMEM supplemented with 10% FBS. Confluent cells were washed twice with PBS and incubated in serum-free DMEM for 24 hours to synchronize the growth potential of the cells. After overnight serum deprivation, cells were treated with LFA (10^{-7} M final concentration) and vehicle control (ethanol, final dilution 1:1000) in DMEM with and without 10% FBS. Cells and conditioned media were harvested 24, 48, and 72 hours after treatment.

Total RNA. Total RNA was isolated using a purification kit (RNeasy Mini Kit; Qiagen, Valencia, CA) according to the manufacturer's protocol. Total RNA (250 ng) was reverse transcribed into cDNA using a cDNA synthesis kit (iScript; Bio-Rad). Quantitative real-time polymerase chain reaction using OPN (forward, 5′-ACAGCCAGGACTCCATTGAC-3′; reverse, 5′-ACACTATCACCTCGGCCATC-3′) and GAPDH (forward, 5′-CCTCTGACTTCAACAGC-3′; reverse, 5′-GCTGTAGCCAAATTCGT-3′) primers was performed (LightCycler 480 SYBR Green Master Kit; Roche) by pre-denaturation at 95°C (1 cycle) followed by amplification (45 cycles): denaturation at 95°C, annealing at 63°C, and extension at 72°C. Fold change was calculated after normalization with GAPDH.

Total Protein. NTM cell pellets were suspended in ice-cold lysis buffer and passed repeatedly through a 21-gauge needle. Lysate was centrifuged at 13,000*g* for 10 minutes, and total protein was quantified by the Bradford assay. Equal protein amounts (15 μg) were separated on 4% to 15% SDS-PAGE gels, transferred to polyvinylidene difluoride membrane, and probed with OPN antibody as described.

Measurement of IOP in *OPN*$^{-/-}$ Mice

Adult *OPN*$^{-/-}$ mice (C57BL/6) and wild-type controls were purchased from the Jackson Laboratory (Bar Harbor, ME). The mice were anesthetized by intraperitoneal injection of a ketamine/xylazine mixture (100 and 9 mg/kg, respectively; Phoenix Pharmaceutical, St. Joseph, MO). A previously validated commercial rebound tonometer (TonoLab; Colonial Medical Supply, Franconia, NH) was used to take three sets of six IOP measurements from each eye.[44,45] Right and left eyes were measured alternatingly, with the initial eye selected randomly. All measurements were taken between 4 and 7 minutes after intraperitoneal injection because previous studies have shown this to be a period with stable IOP.[12,46,47] As indicated by the manufacturer, the tonometer (TonoLab; Colonial Medical Supply) was fixed horizontally for all measurements, and the tip of the probe was placed 2 to 3 mm from the eye. To reduce variability in measurements, the tonometer was modified to include a pedal that activated the probe without the need to handle the device. The probe contacted the eye perpendicularly over the central cornea. Verification of targeting was performed under direct visualization using 5.5× magnification. The average of a set of measurements for each eye was accepted only if the device indicated that there was "no significant variability" (per the protocol manual; Colonial Medical Supply). Measurements were taken at the age of 7 weeks between 11:00 and 15:00 hours to minimize the effect of diurnal variation.

Measurement of Central Corneal Thickness

In humans, contact tonometry measurements by variable force spring tonometers (e.g., Goldmann, Tono-Pen) may be affected by central corneal thickness.[48] To assess whether this confounder contributes to any observed IOP difference, the central corneal thickness of 6.5-week-old *OPN*$^{-/-}$ and wild-type mice were measured using optical coherence tomography (Stratus; Carl Zeiss Meditec, Inc., Dublin, CA). The mice were imaged with optical coherence tomography under anesthesia (ketamine/xylazine mixture). Central corneal thickness was obtained by using the internal software (version 4.0.7) and measuring the distance between the epithelial and endothelial peak amplitudes.[12]

Histology

Eyes were enucleated from euthanatized 8-week-old wild-type and *OPN*$^{-/-}$ mice and were placed in 2.5% glutaraldehyde/2% formaldehyde in 0.1 M cacodylate buffer containing 0.08 M $CaCl_2$ at 4°C for 20 minutes.[12] After incubation, eyes were hemisected, and the tissue minus the lens was returned to fixative for 24 hours. Tissue was postfixed for 1.5 hours in 2% aqueous OsO_4. Tissue was dehydrated in graded concentrations of ethanol, transitioned in propylene oxide, infiltrated with propylene oxide and Epon mixtures (TAAB 812 resin; Marivac, Quebec, Canada), embedded in Epon, and cured for 48 hours at 60°C. Sections (1 μm) were stained with 1% toluidine blue in 1% borate buffer.

Statistical Analysis

Results are expressed as mean ± SD. Data from various experimental and control groups were compared using Student's unpaired *t*-test. Differences were considered significant when $P < 0.05$.

Results

Expression of OPN in Normal and POAG Human AH

Previous proteomic studies from our laboratory have shown high levels of OPN in human AH.[40] To validate this, OPN was evaluated in donor POAG and normal AH by ELISA. In AH obtained from donor eyes, POAG OPN levels (normalized to total protein concentration) were significantly lower than normal (0.54 ± 0.18 ng/μg vs. 0.77 ± 0.23 ng/μg; $P = 0.039$; Fig. 1A). No statistical difference between total protein of donor POAG and normal AH was observed (0.929 ± 0.28 μg/μL vs. 0.919 ± 0.29 μg/μL; $P = 0.96$). When analyzed by volume, OPN concentration was also found to be significantly lower in donor POAG AH compared with normal AH (0.5 ± 0.18 ng/μL vs.0.67 ± 0.14 ng/μL; $P = 0.044$).

OPN levels in AH obtained during surgery showed a similar trend to OPN levels in donor eyes. In surgical POAG AH, OPN levels (normalized to total protein concentration) were lower than in AH from elective cataract controls (1.05 ng/μg vs.1.43 ng/μg; $P = 0.083$; Fig. 1B). No significant change in OPN concentration by volume was noted between surgical POAG and elective cataract control AH samples (0.27 ± 0.09 ng/μL vs. 0.26 ± 0.16 ng/μL; $P = 0.80$). However, total protein concentration was significantly higher in surgical POAG AH than in elective cataract control AH (0.265 ± 0.08 μg/μL vs. 0.195 ± 0.09 μg/μL; $P = 0.005$).

To confirm the ELISA results, Western blot analysis was performed on POAG and normal AH obtained from donor eyes. Using

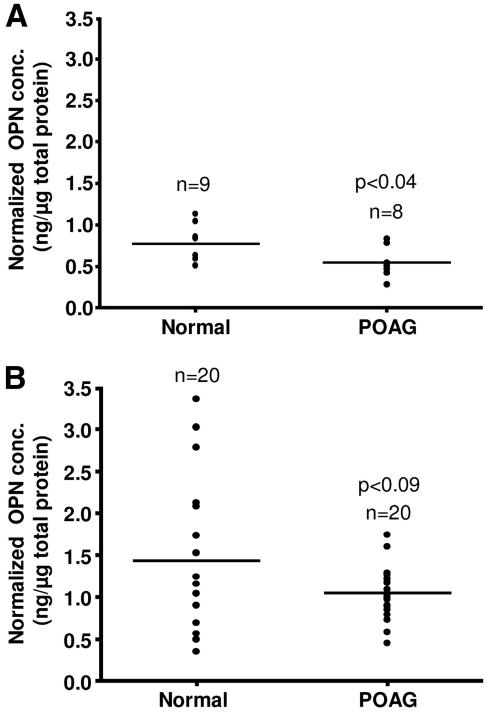

FIGURE 1. OPN concentration in donor and surgical AH. OPN concentrations are reduced in (**A**) donor and (**B**) surgical AH derived from POAG when compared with normal or elective cataract controls.

an anti–OPN polyclonal antibody, six OPN protein products were detected (Fig. 2A). Results show a wide variation in OPN expression profiles within POAG and normal samples. Interestingly, OPN band 4 (70 kDa) was found to be absent in 3 of the 6 POAG samples (Fig. 2A, lanes 10, 12, 13). Although band 4 was present in all normal samples, reduced expression was noted in 2 of the 8 samples (Fig. 2A, lanes 4 and 5). The mean intensity of individual bands 1 to 5 (normalized to HAS) was found to be lower in POAG than in normal (Fig. 2B) AH. Conversely, band 6 was slightly higher in POAG than in normal AH. Only band 2 was found to be significantly different between POAG and normal AH ($P < 0.02$). When the intensity of all six bands was combined, POAG samples had lower OPN expression than normal samples, consistent with ELISA results (Fig. 1).

Evaluation of OPN Expression in Ocular Tissues by Immunohistochemistry

Because several components of AH are actively secreted by eye tissues,[40,49] there is a high probability that OPN is synthesized by eye tissues themselves. To analyze this, we evaluated the presence of OPN by immunohistochemistry in various ocular tissues. Using a monoclonal anti–OPN antibody, OPN staining was shown to be present in the trabecular meshwork, corneal epithelium and endothelium, iris, ciliary body, retina and anterior and posterior optic nerves (Fig. 3).

OPN Expression Pattern in Various Ocular Tissues

The expression profile of OPN was further evaluated by Western blot analysis in iris, retina, optic nerve, vitreous humor, and trabecular meshwork obtained from three normal donor eyes (Fig. 4). Although there was variation in OPN expression among the samples, it was found to be strongly expressed in retina, trabecular meshwork, and optic nerve, confirming expression studies performed by immunohistochemistry. Only 1 of 3 samples showed OPN in the iris, and 2 of 3 samples showed OPN in vitreous humor.

OPN protein size also varied among tissues (Fig. 4). In retina and vitreous humor, a doublet was observed at approximately 55 kDa. In the TM, OPN was present as a single band at 55 kDa. OPN expression in optic nerve varied in each sample, appearing as either a singlet or a doublet at 55 kDa. Smaller molecular weight OPN proteins were identified in the retina (35 kDa, 26 kDa, 25 kDa), optic nerve (35 kDa), and vitreous (35 kDa, 26 kDa).

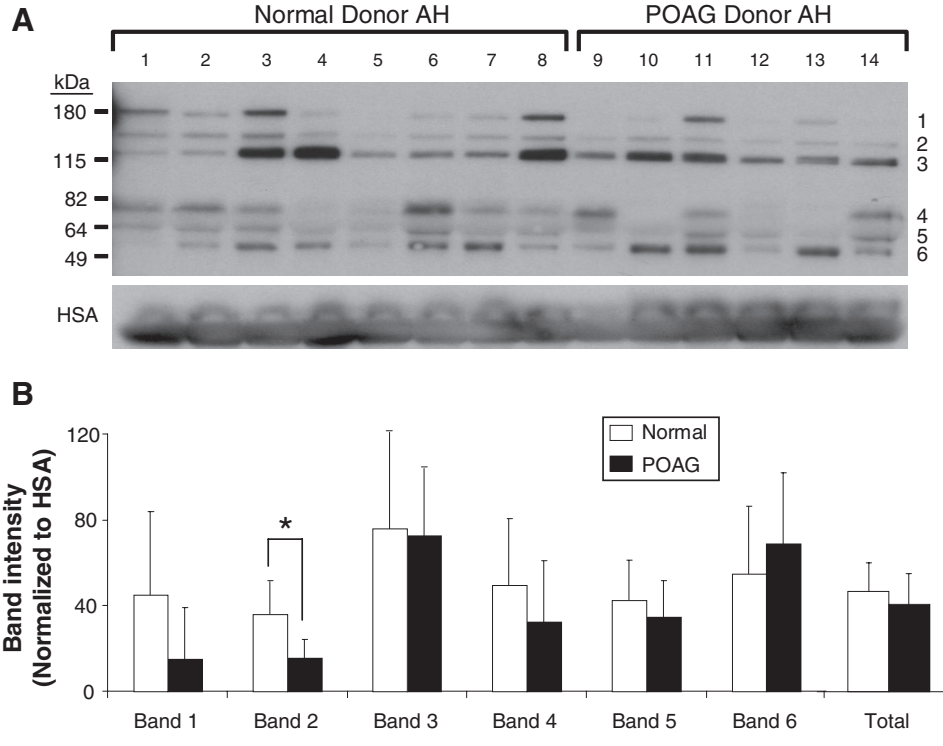

FIGURE 2. OPN expression in normal and POAG AH. (**A**) Western blot shows six OPN protein molecular weights. The 70-kDa OPN protein (band 4) was absent in 3 of the 6 POAG samples. (**B**) Densitometric analysis of OPN bands 1 to 5 show decreased OPN in POAG compared with normal. Only band 6 shows an increase of OPN in POAG. Total OPN protein was lower in POAG than in normal AH. Human serum albumin (HSA) was used for internal AH control and to normalize each band intensity. $^*P < 0.02$.

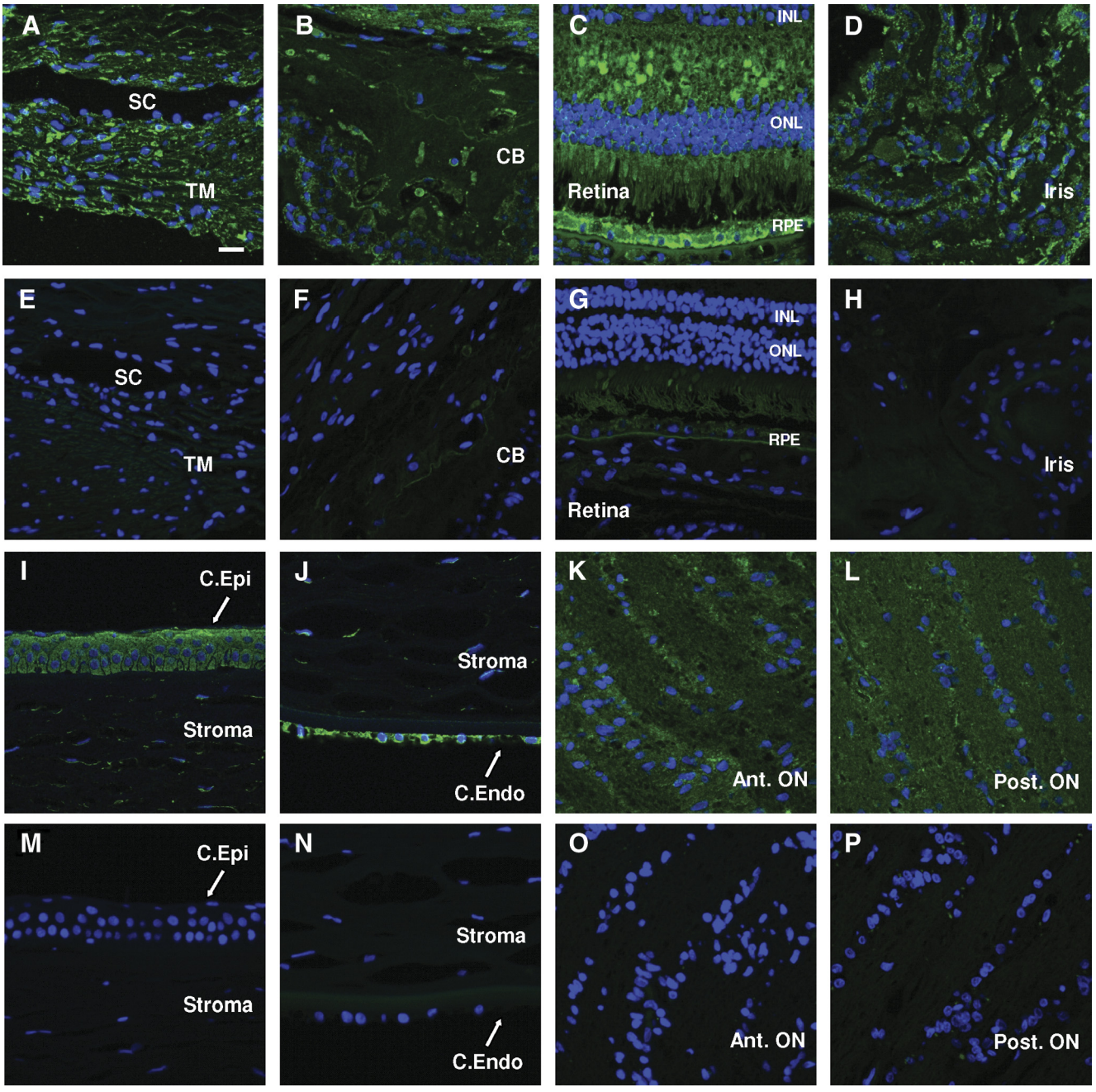

FIGURE 3. OPN expression in different ocular tissues. (**A–D**, **I–L**) Immunofluorescence and subsequent confocal microscopy show strong expression and localization of OPN in eye tissues within both anterior and posterior chambers. (**E–H**, **M–P**) Secondary antibody alone controls are shown for comparison. (**A**, **E**) Trabecular meshwork (TM). (**B**, **F**) Ciliary body (CB). (**C**, **G**) Retina. (**D**, **H**) Iris. (**I**, **M**) Corneal epithelium (C. Epi). (**J**, **N**) Corneal endothelium (C. Endo). (**K**, **O**) Anterior optic nerve (Ant ON). (**L**, **P**) Posterior optic nerve (Post ON). RPE, retinal pigment epithelium; ONL, outer nuclear layer; INL, inner nuclear layer; SC, Schlemm's canal. Image exposure for an eye tissue was the same as the corresponding negative control. Pictures are representative of OPN staining performed in three sections obtained from two donor eyes. Scale bar, 10 μm.

Evaluation of OPN Glycosylation in POAG and Normal AH

We hypothesized that at least some of the multiple OPN bands were attributed to differential glycosylation of the protein because several investigators have shown extensive glycosylation in OPN.[50,51] Enzymatic deglycosylation of the protein component in AH from normal and POAG donor eyes showed a downward shift of several OPN bands by Western blot (Fig. 5A). This suggests that several glycosylated products of OPN are present in AH. In contrast, enzymatic deglycosylation of optic nerve and TM lysate showed no change in OPN migration in POAG and normal samples, indicating a lack of glycosylation (Fig. 5B).

Evaluation of OPN Expression in Response to LFA in Cultured NTM Cells

One of the limitations of studying proteins in POAG AH is that most of the samples are from patients who are on pressure-lowering medications such as prostaglandin analogs. To deter-

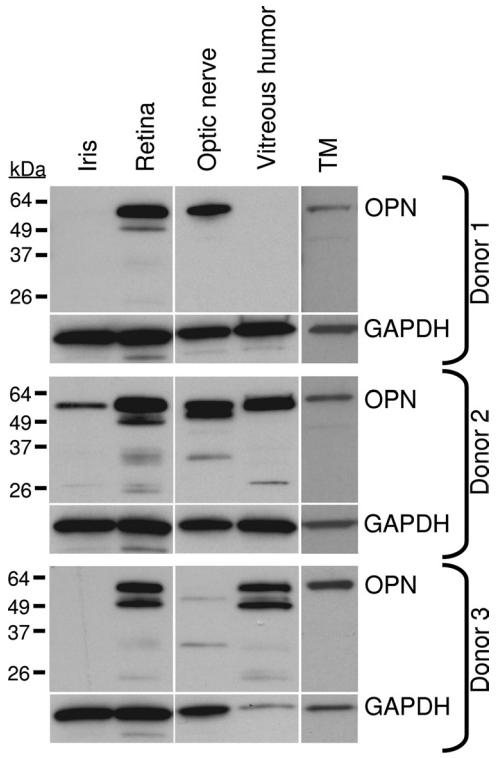

FIGURE 4. Western blot analysis of OPN in ocular tissues. Considerable variation in OPN expression profile was seen across different ocular samples. OPN was consistently found in retina, optic nerve, and trabecular meshwork (TM). OPN was also identified in iris and vitreous humor in at least 1 of the 3 samples.

mine whether prostaglandin analogs affect the expression of OPN, overnight serum-deprived NTM cells were treated with LFA or vehicle in DMEM with or without 10% FBS. In serum-containing media, *OPN* mRNA levels were increased at 24 (6.5 ± 0.5-fold; $n = 3$) and 48 (3.7 ± 2.0-fold; $n = 3$) hours compared with vehicle control (Fig. 6A). Conversely, LFA treatment of NTM cells in serum-free media did not change *OPN* gene expression (Fig. 6B). GAPDH mRNA expression (internal control) was not altered by LFA treatment with or without 10% FBS over the same time course (data not shown). Western blot analysis of lysates from cells treated with LFA for 24 and 48 hours in 10% FBS-containing media showed no change in OPN protein expression (Fig. 6C). Similarly, conditioned media (containing 10% FBS) from LFA-treated NTM cells showed no change in secreted OPN over the same time course (Fig. 6D). A slight increase in OPN expression in conditioned media was noted at 72 hours after treatment (Fig. 6D).

Effect of *OPN* Gene Knockout on IOP

Given that OPN was differentially expressed in POAG AH and SPARC$^{-/-}$ mice had lower IOP than littermate controls,[12] we investigated whether the lack of OPN had any effect on IOP. Analysis of IOP in 7-week-old *OPN*$^{-/-}$ mice showed no difference in IOP when compared with wild-type controls (17.5 ± 2.0 mm Hg [$n = 56$] vs. 17.3 ± 1.9 mm Hg [$n = 68$]). Optical coherence tomography showed *OPN*$^{-/-}$ mice had thinner central corneal thickness than did wild-type control (91.7 ± 3.6 μm [$n = 50$] vs. 99.2 ± 5.5 μm [$n = 70$]; $P > 0.001$). There were no observable anatomic differences within the outflow tissues between the wild-type and the *OPN*$^{-/-}$ mice at the light microscopy level (Fig. 7).

DISCUSSION

IOP regulation within the human eye occurs primarily in the conventional outflow pathway, where cellular components of the trabecular meshwork and Schlemm's canal work in conjunction with the ECM to regulate AH removal from the anterior segment. Associated with the interplay between the cells and the extracellular matrix are matricellular proteins. SPARC, a member of the matricellular protein family, has been shown to be directly involved in IOP regulation.[12] Conversely, hevin, a close homolog of SPARC, does not have a direct effect on IOP.[52] In this study, we found the matricellular protein OPN to be expressed at lower levels in POAG AH than in controls. Variation in OPN protein size was observed in POAG AH. Some, but not all, of the OPN size variation was due to glycosylation. However, unlike *SPARC*$^{-/-}$ mice, we did not observe any significant difference in IOP of *OPN*$^{-/-}$ mice when compared with wild-type controls.

Our study indicates a decreasing trend of OPN in POAG AH, whereas other matricellular proteins are reported to be upregulated at the mRNA level in POAG after mechanical stretch or in response to elevated IOP.[22,53,54] The reason for decreased OPN levels in POAG AH is unknown. Previous studies evaluating gene expression profiles of human TM cells in response to glaucomatous insults such as dexamethasone treatment did not find upregulation of the *OPN* gene.[55,56] However, contrasting reports from nonocular cells (osteoprecursor and lung cells) suggest that dexamethasone treatment may affect *OPN* gene expression in a cell type–specific manner.[57,58] Unlike other matricellular proteins, OPN is an inhibitor of calcification and aids in the dissolution of mineral deposits.[59,60] Matrix Gla protein, another inhibitor of calcification, is decreased in the TMs isolated from POAG patients.[38] With OPN decreased in POAG AH and matrix Gla protein reduced in POAG TMs, it is

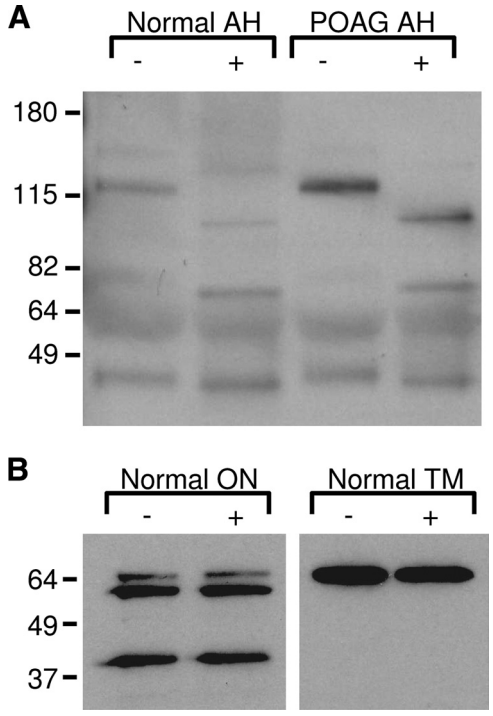

FIGURE 5. Deglycosylation of OPN. (**A**) After deglycosylation (+), OPN protein fragments appeared as lower molecular weights compared with nondeglycosylated controls (−). (**B**) No change in OPN migration was observed when optic nerve (ON) or normal trabecular meshwork (TM) tissue was treated with (+) or without (−) glycosidases.

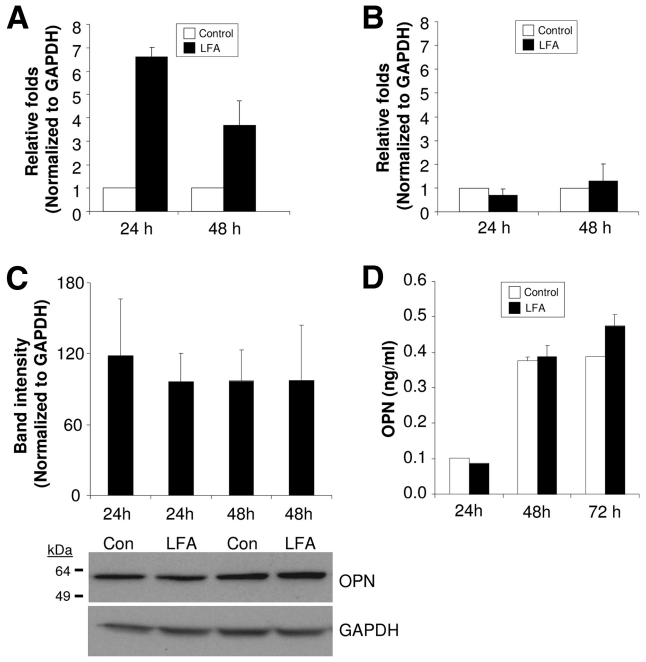

FIGURE 6. Effect of LFA on *OPN* gene expression in primary NTM cells. (**A**) *OPN* mRNA induction increased within 24 hours after LFA treatment in 10% FBS-containing media. (**B**) No changes in *OPN* mRNA level were identified when NTM cells remained in serum-free conditions. (**C**) Intracellular and (**D**) secreted OPN protein levels did not change within 48 hours after LFA treatment in 10% FBS-containing media. A slight increase (20%) in secreted OPN was found at 72 hours but was not significant.

tempting to speculate that a decrease in calcification inhibitors may lead to an increase in TM mineralization. Normally, the trabecular meshwork is a spongiform tissue that reacts to various forms of stress (e.g., shear, stretch) to modulate outflow. An increase in mineralization may result in a TM that is stiffer and less responsive to stress, leading to decreased outflow and elevated IOP. Last et al.[39] reported that the TM is less pliable and stiffer in POAG than in age-matched normal controls, supporting this concept.

Another possibility for lower OPN levels in POAG AH may be the presence of a negative feedback loop by which the eye responds to increased IOP.[61,62] Matricellular proteins have often been shown to be expressed in an opposing manner in physiological or pathologic processes. In the case of non–small cell lung cancer, increased OPN favored progression of the disease but was accompanied by a lower expression of SPARC.[61] In addition, overexpression of *OPN* mRNA has been linked to a poor prognosis for ovarian cancer patients, whereas overexpression of SPARC protein in an ovarian carcinoma cell line is inversely correlated with the degree of malignancy by promoting apoptosis, indicating a tumor suppressor role for SPARC in these cells.[62]

Contradictory to our results is the finding of increased OPN in the AH of DBA2/J mice.[63] Although this may be explained by the differences between humans and mice, it may also represent a difference in the etiology of the glaucoma. In DBA2/J mice, elevated IOP is caused by the shedding of pigment from the iris, resulting in a significant inflammatory response and eventual neovascular scarring of the angle. In POAG, pigment is generally not a factor, but the etiology of elevated IOP is unknown.

Our finding of upregulated *OPN* mRNA in response to LFA treatment corroborates a previous report showing prostaglandin treatment increased *OPN* gene expression in human adipose tissue–derived mesenchymal stem cells.[64] In our study, we observed an increase in *OPN* mRNA after LFA treatment. However, we did not observe a change in OPN protein expression within 48 hours of LFA treatment (cellular or secreted). Only at 72 hours after treatment did we see a slight increase in OPN secretion. This suggests that LFA does not contribute to the lower OPN concentrations seen in POAG AH. Interestingly, we could induce an increase in *OPN* gene transcription only in NTM cells treated with LFA in serum-containing media. Whether LFA needed auxiliary proteins from the FBS to induce *OPN* transcription is unknown.

In humans, OPN is found in many tissues and almost all body fluids, including blood, urine, and milk.[65] Extensive posttranslational modifications affect OPN function in a tissue-specific manner.[50] In AH, six different OPN products were identified; sizes ranged from 55 to 180 kDa. OPN is glycosylated in AH, but these modifications do not account for all the OPN size variations. In addition to glycosylation, OPN is posttranslationally modified by sulfation, serine/threonine phosphorylation, sialylation, and transglutamination.[50,66–68] The higher molecular weight bands (>55 kDa) we observed in AH corroborate with similarly sized OPN fragments found in bone lysate and calcified arteries of mice.[68,69] Bands 4 and 5 correspond to full-length OPN (Fig. 2). Reduction of band 4 in POAG AH suggests a loss of OPN full-length biological function. The remaining bands are smaller than full-length OPN, consistent with cleaved products. OPN has been shown to be cleaved by a variety of molecules, including thrombin, plasmin, cathepsin D, and various matrix metalloproteinases s.[65,70–72] The importance of the smaller fragments are unknown. Given the inadequate understanding of the pathophysiology of glaucoma, it is difficult to say whether changes in OPN are the cause or the effect of the disease itself. Further experiments are required to

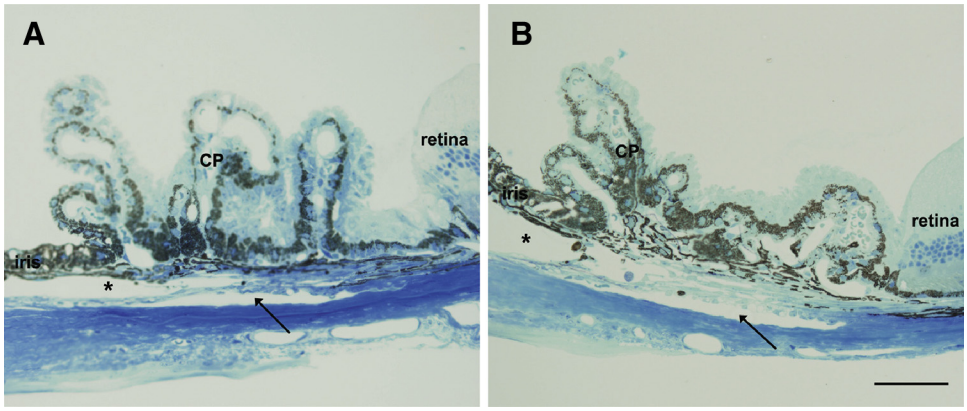

FIGURE 7. Iridocorneal angles of wild-type and $OPN^{-/-}$ mice. Iridocorneal angles of (**A**) 8-week-old wild-type and (**B**) age-matched $OPN^{-/-}$ mice appeared microscopically indistinguishable. Schlemm's canal, trabecular beams, cellularity, uveoscleral outflow pathway, and ciliary body location all appeared normal. CP, ciliary processes. *Asterisk*: anterior chamber; *arrow*: Schlemm's canal. Scale bar, 50 μm.

determine the biological function of OPN in normal AH and the consequence of reduction in several OPN fragments.

In eye tissues, differences in OPN banding patterns were also noted in trabecular meshwork, iris, optic nerve, retina, vitreous humor, and AH. In trabecular meshwork, OPN was seen as a single band found at 55 kDa. Although the 55-kDa band was consistent between all the tissues analyzed, a doublet was found in the retina, optic nerve, and vitreous humor in at least 1 of the 3 samples studied. The observed differences in OPN expression in different eye tissues may indicate active synthesis of the protein and may contribute to the total secreted OPN in AH. However, the contribution of OPN via serum (at least for some of the OPN forms or part of the total OPN) cannot be ruled out.

Wild-type mice have a wide range of baseline IOP (4–20 mm Hg) that is strain dependent.[12,44,63,73,74] Thus, it is important that comparative studies, such as ours, use paired wild-type and knockout mice from the same background strain. Unlike $SPARC^{-/-}$ mice, which had lower IOP than wild-type controls,[12] the $OPN^{-/-}$ mice did not show any change in IOP compared with controls. $OPN^{-/-}$ mice did, however, have a 7.6% thinner central corneal thickness. In humans, a 10% change in central corneal thickness is generally considered significant using Goldmann applanation tonometry. However, our calibration with manometry indicates that central corneal thickness does not appear to have a significant impact with rebound tonometry.[48] Previous studies in mice found a high correlation between the IOPs measured by tonometer and manometry. This suggests that central corneal thickness does not affect IOP measurements using rebound tonometry.[63,74] Taken together, these results indicate that there may not be a direct involvement of OPN in IOP regulation in young mice.

In summary, our results demonstrate a strong presence of OPN in various tissues of the eye and an overall decrease of OPN in POAG AH compared with control AH. Further studies are required to specifically determine whether OPN can be used as a potential marker for POAG.

References

1. Grant WM. Experimental aqueous perfusion in enucleated human eyes. *Arch Ophthalmol.* 1963;69:783–801.
2. Acott TS, Kelley MJ. Extracellular matrix in the trabecular meshwork. *Exp Eye Res.* 2008;86:543–561.
3. Tamm ER, Fuchshofer R. What increases outflow resistance in primary open-angle glaucoma? *Surv Ophthalmol.* 2007;52(suppl 2):S101–S104.
4. Bahler CK, Howell KG, Hann CR, Fautsch MP, Johnson DH. Prostaglandins increase trabecular meshwork outflow facility in cultured human anterior segments. *Am J Ophthalmol.* 2008;145:114–119.
5. Oh D-J, Martin JL, Williams AJ, Russell P, Birk DE, Rhee DJ. Effect of latanoprost on the expression of matrix metalloproteinases and their tissue inhibitors in human trabecular meshwork cells. *Invest Ophthalmol Vis Sci*. 2006;47:3887–3895.
6. Sagara T, Gaton DD, Lindsey JD, Gabelt BT, Kaufman PL, Weinreb RN. Topical prostaglandin F2 treatment reduces collagen types I, III, and IV in the monkey uveoscleral outflow pathway. *Arch Ophthalmol.* 1999;117:794–801.
7. Toris CB, Gabelt BT, Kaufman PL. Update on the mechanism of action of topical prostaglandins for intraocular pressure reduction. *Surv Ophthalmol.* 2008;53:S107–S120.
8. Denhardt DT, Giachelli CM, Rittling SR. Role of osteopontin in cellular signaling and toxicant injury. *Annu Rev Pharmacol Toxicol.* 2001;41:723–749.
9. Denhardt DT, Noda M, O'Regan AW, Pavlin D, Berman JS. Osteopontin as a means to cope with environmental insults: regulation of inflammation, tissue remodeling, and cell survival. *J Clin Invest.* 2001;107:1055–1061.
10. Rhee DJ, Haddadin RI, Kang MH, Oh DJ. Matricellular proteins in the trabecular meshwork. *Exp Eye Res.* 2009;88:694–703.
11. Sodek J, Batista Da Silva AP, Zohar R. Osteopontin and mucosal protection. *J Dent Res.* 2006;85:404–415.
12. Haddadin RI, Oh DJ, Kang MH, et al. SPARC-null mice exhibit lower intraocular pressures. *Invest Ophthalmol Vis Sci.* 2009;50:3771–3777.
13. Li Y, Aroca-Aguilar JD, Ghosh S, Sanchez-Sanchez F, Escribano J, Coca-Prados M. Interaction of myocilin with the C-terminal region of hevin. *Biochem Biophys Res Commun.* 2006;339:797–804.
14. Kirwan RP, Wordinger RJ, Clark AF, O'Brien CJ. Differential global and extra-cellular matrix focused gene expression patterns between normal and glaucomatous human lamina cribrosa cells. *Mol Vis.* 2009;15:76–88.
15. Fuchshofer R, Tamm ER. Modulation of extracellular matrix turnover in the trabecular meshwork. *Exp Eye Res.* 2009;88:683–688.
16. Inatani M, Tanihara H, Katsuta H, Honjo M, Kido N, Honda Y. Transforming growth factor-beta 2 levels in aqueous humor of glaucomatous eyes. *Graefes Arch Clin Exp Ophthalmol.* 2001;239:109–113.
17. Ochiai Y, Ochiai H. Higher concentration of transforming growth factor-beta in aqueous humor of glaucomatous eyes and diabetic eyes. *Jpn J Ophthalmol.* 2002;46:249–253.
18. Picht G, Welge-Luessen U, Grehn F, Lutjen-Drecoll E. Transforming growth factor beta 2 levels in the aqueous humor in different types of glaucoma and the relation to filtering bleb development. *Graefes Arch Clin Exp Ophthalmol.* 2001;239:199–207.
19. Tripathi RC, Li J, Chan WF, Tripathi BJ. Aqueous humor in glaucomatous eyes contains an increased level of TGF-beta 2. *Exp Eye Res.* 1994;59:723–727.
20. Chiquet-Ehrismann R. Tenascins. *Int J Biochem Cell Biol.* 2004;36:986–990.
21. Chiquet-Ehrismann R, Chiquet M. Tenascins: regulation and putative functions during pathological stress. *J Pathol.* 2003;200:488–499.
22. Keller KE, Kelley MJ, Acott TS. Extracellular matrix gene alternative splicing by trabecular meshwork cells in response to mechanical stretching. *Invest Ophthalmol Vis Sci.* 2007;48:1164–1172.
23. Duvall CL, Taylor WR, Weiss D, Wojtowicz AM, Guldberg RE. Impaired angiogenesis, early callus formation, and late stage remodeling in fracture healing of osteopontin-deficient mice. *J Bone Miner Res.* 2007;22:286–297.
24. Giachelli CM, Steitz S. Osteopontin: a versatile regulator of inflammation and biomineralization. *Matrix Biol.* 2000;19:615–622.
25. Klingel K, Kandolf R. Osteopontin: a biomarker to predict the outcome of inflammatory heart disease. *Semin Thromb Hemost.* 2010;36:195–202.
26. Waller AH, Sanchez-Ross M, Kaluski E, Klapholz M. Osteopontin in cardiovascular disease: a potential therapeutic target. *Cardiol Rev.* 2010;18:125–131.
27. Scatena M, Liaw I, Giachelli CM. Osteopontin: a multifunctional molecule regulating chronic inflammation and vascular disease. *Arterioscler Thromb Vasc Biol.* 2007;27:2302–2309.
28. Uede T, Katagiri Y, Iizuka J, Murakami M. Osteopontin, a coordinator of host defense system: acytokine or an extracellular matrix adhesive protein. *Microbiol Immunol.* 1997;41:641–648.
29. Wang KX, Denhardt DT. Osteopontin: role in immune regulation and stress responses. *Cytokine Growth Factor Rev.* 2008;19:333–345.
30. Chidlow G, Wood JP, Manavis J, Osborne NN, Casson RJ. Expression of osteopontin in the rat retina: effects of excitotoxic and ischemic injuries. *Invest Ophthalmol Vis Sci.* 2008;49:762–771.
31. Fujita N, Fujita S, Okada Y, et al. Impaired angiogenic response in the corneas of mice lacking osteopontin. *Invest Ophthalmol Vis Sci.* 2010;51:790–794.
32. Miyazaki K, Okada Y, Yamanaka O, et al. Corneal wound healing in an osteopontin-deficient mouse. *Invest Ophthalmol Vis Sci.* 2008;49:1367–1375.
33. Saika S, Shirai K, Yamanaka O, et al. Loss of osteopontin perturbs the epithelial-mesenchymal transition in an injured mouse lens epithelium. *Lab Invest.* 2007;87:130–138.

34. Gonzalez P, Epstein DL, Borras T. Characterization of gene expression in human trabecular meshwork using single-pass sequencing of 1060 clones. *Invest Ophthalmol Vis Sci.* 2000;41:3678–3693.
35. Gonzalez P, Zigler JS Jr, Epstein DL, Borras T. Identification and isolation of differentially expressed genes from very small tissue samples. *BioTechniques.* 1999;26:884–886, 888–892.
36. Tomarev SI, Wistow G, Raymond V, Dubois S, Malyukova I. Gene expression profile of the human trabecular meshwork: NEIBank sequence tag analysis. *Invest Ophthalmol Vis Sci.* 2003;44:2588–2596.
37. Borras T, Comes N. Evidence for a calcification process in the trabecular meshwork. *Exp Eye Res.* 2009;88:738–746.
38. Xue W, Comes N, Borras T. Presence of an established calcification marker in trabecular meshwork tissue of glaucoma donors. *Invest Ophthalmol Vis Sci.* 2007;48:3184–3194.
39. Last JA, Pan T, Ding Y, et al. Elastic modulus determination of normal and glaucomatous human trabecular meshwork. *Invest Ophthalmol Vis Sci.* 2011;52:2147–2152.
40. Chowdhury UR, Madden BJ, Charlesworth MC, Fautsch MP. Proteome analysis of human aqueous humor. *Invest Ophthalmol Vis Sci.* 2010;51:4921–4931.
41. Ezzat MK, Howell KG, Bahler CK, et al. Characterization of monoclonal antibodies against the glaucoma-associated protein myocilin. *Exp Eye Res.* 2008;87:376–384.
42. Fautsch MP, Bahler CK, Jewison DJ, Johnson DH. Recombinant TIGR/MYOC increases outflow resistance in the human anterior segment. *Invest Ophthalmol Vis Sci.* 2000;41:4163–4168.
43. Stamer WD, Seftor RE, Williams SK, Samaha HA, Snyder RW. Isolation and culture of human trabecular meshwork cells by extracellular matrix digestion. *Curr Eye Res.* 1995;14:611–617.
44. Saeki T, Aihara M, Ohashi M, Araie M. The efficacy of TonoLab in detecting physiological and pharmacological changes of mouse intraocular pressure: comparison with TonoPen and microneedle manometry. *Curr Eye Res.* 2008;33:247–252.
45. Wang WH, Millar JC, Pang IH, Wax MB, Clark AF. Noninvasive measurement of rodent intraocular pressure with a rebound tonometer. *Invest Ophthalmol Vis Sci.* 2005;46:4617–4621.
46. Aihara M, Lindsey JD, Weinreb RN. Reduction in intraocular pressure in mouse eyes treated with latanoprost. *Invest Ophthalmol Vis Sci.* 2002;43:146–150.
47. Savinova OV, Sugiyama F, Martin JE, et al. Intraocular pressure in genetically distinct mice: an update and strain survey. *BMC Genet.* 2001;2:12.
48. Brandt JD. Corneal thickness in glaucoma screening, diagnosis, and management. *Curr Opin Ophthalmol.* 2004;15:85–89.
49. Escribano J, Ortego J, Coca-Prados M. Isolation and characterization of cell-specific cDNA clones from a subtractive library of the ocular ciliary body of a single normal human donor: transcription and synthesis of plasma proteins. *J Biochem.* 1995;118:921–931.
50. Kazanecki CC, Uzwiak DJ, Denhardt DT. Control of osteopontin signaling and function by post-translational phosphorylation and protein folding. *J Cell Biochem.* 2007;102:912–924.
51. Singh K, DeVouge MW, Mukherjee BB. Physiological properties and differential glycosylation of phosphorylated and nonphosphorylated forms of osteopontin secreted by normal rat kidney cells. *J Biol Chem.* 1990;265:18696–18701.
52. Kang MH, Oh DJ, Rhee DJ. Effect of hevin deletion in mice and characterization in trabecular meshwork. *Invest Ophthalmol Vis Sci.* 2011;52:2187–2193.
53. Flugel-Koch C, Ohlmann A, Fuchshofer R, Welge-Lussen U, Tamm ER. Thrombospondin-1 in the trabecular meshwork: localization in normal and glaucomatous eyes, and induction by TGF-b1 and dexamethasone in vitro. *Exp Eye Res.* 2004;79:649–663.
54. Johnson EC, Jia L, Cepurna WO, Doser TA, Morrison JC. Global changes in optic nerve head gene expression after exposure to elevated intraocular pressure in a rat glaucoma model. *Invest Ophthalmol Vis Sci.* 2007;48:3161–3177.
55. Fan BJ, Wang DY, Tham CC, Lam DS, Pang CP. Gene expression profiles of human trabecular meshwork cells induced by triamcinolone and dexamethasone. *Invest Ophthalmol Vis Sci.* 2008;49:1886–1897.
56. Rozsa FW, Reed DM, Scott KM, et al. Gene expression profile of human trabecular meshwork cells in response to long-term dexamethasone exposure. *Mol Vis.* 2006;12:125–141.
57. Kurokawa M, Konno S, Matsukura S, et al. Effects of corticosteroids on osteopontin expression in a murine model of allergic asthma. *Int Arch Allergy Immunol.* 2009;149(suppl 1):7–13.
58. Park JB. The effects of dexamethasone, ascorbic acid, and beta-glycerophosphate on osteoblastic differentiation by regulating estrogen receptor and osteopontin expression. *J Surg Res.* In press.
59. Giachelli CM. Inducers and inhibitors of biomineralization: lessons from pathological calcification. *Orthod Craniofac Res.* 2005;8:229–231.
60. Steitz SA, Speer MY, McKee MD, et al. Osteopontin inhibits mineral deposition and promotes regression of ectopic calcification. *Am J Pathol.* 2002;161:2035–2046.
61. Schneider S, Yochim J, Brabender J, et al. Osteopontin but not osteonectin messenger RNA expression is a prognostic marker in curatively resected non-small cell lung cancer. *Clin Cancer Res.* 2004;10:1588–1596.
62. Yiu GK, Chan WY, Ng SW, et al. SPARC (secreted protein acidic and rich in cysteine) induces apoptosis in ovarian cancer cells. *Am J Pathol.* 2001;159:609–622.
63. Birke MT, Neumann C, Birke K, Kremers J, Scholz M. Changes of osteopontin (OPN) in the aqueous humor of the DBA2/J glaucoma model correlated with optic nerve and RGC degenerations. *Invest Ophthalmol Vis Sci.* 2010;51:5759–5767.
64. Knippenberg M, Helder MN, de Blieck-Hogervorst JM, Wuisman PI, Klein-Nulend J. Prostaglandins differentially affect osteogenic differentiation of human adipose tissue-derived mesenchymal stem cells. *Tissue Eng.* 2007;13:2495–2503.
65. Christensen B, Schack L, Klaning E, Sorensen ES. Osteopontin is cleaved at multiple sites close to its integrin-binding motifs in milk and is a novel substrate for plasmin and cathepsin D. *J Biol Chem.* 2010;285:7929–7937.
66. Beninati S, Senger DR, Cordella-Miele E, et al. Osteopontin: its transglutaminase-catalyzed posttranslational modifications and cross-linking to fibronectin. *J Biochem.* 1994;115:675–682.
67. Christensen B, Nielsen MS, Haselmann KF, Petersen TE, Sorensen ES. Post-translationally modified residues of native human osteopontin are located in clusters: identification of 36 phosphorylation and five O-glycosylation sites and their biological implications. *Biochem J.* 2005;390:285–292.
68. Miwa HE, Gerken TA, Jamison O, Tabak LA. Isoform-specific O-glycosylation of osteopontin and bone sialoprotein by polypeptide N-acetylgalactosaminyltransferase-1. *J Biol Chem.* 2010;285:1208–1219.
69. Kaartinen MT, Murshed M, Karsenty G, McKee MD. Osteopontin upregulation and polymerization by transglutaminase 2 in calcified arteries of matrix Gla protein-deficient mice. *J Histochem Cytochem.* 2007;55:375–386.
70. Agnihotri R, Crawford HC, Haro H, Matrisian LM, Havrda MC, Liaw L. Osteopontin, a novel substrate for matrix metalloproteinase-3 (stromelysin-1) and matrix metalloproteinase-7 (matrilysin). *J Biol Chem.* 2001;276:28261–28267.
71. Senger DR, Perruzzi CA, Papadopoulos A. Elevated expression of secreted phosphoprotein I (osteopontin, 2ar) as a consequence of neoplastic transformation. *Anticancer Res.* 1989;9:1291–1299.
72. Senger DR, Perruzzi CA, Papadopoulos A, Tenen DG. Purification of a human milk protein closely similar to tumor-secreted phosphoproteins and osteopontin. *Biochim Biophys Acta.* 1989;996:43–48.
73. Aihara M, Lindsay JD, Weinreb RN. Aqueous humor dynamics in mice. *Invest Ophthalmol Vis Sci.* 2003;55:5168–5173.
74. Nissirios N, Goldblum D, Rohrer K, Mittag T, Danias J. Noninvasive determination of intraocular pressure (IOP) in nonsedated mice of 5 different inbred strains *J Glaucoma.* 2007;16:57–61.